JOURNAL OF VIROLOGY, Dec. 2004, p. 12747–12761 Vol. 78, No. 23
0022-538X/04/$08.00+0 DOI: 10.1128/JVI.78.23.12747–12761.2004

Resistance to Vesicular Stomatitis Virus Infection Requires a Functional Cross Talk between the Eukaryotic Translation Initiation Factor 2α Kinases PERK and PKR

Dionissios Baltzis,[1] Li-Ke Qu,[1] Stavroula Papadopoulou,[1] Jaime D. Blais,[2] John C. Bell,[2] Nahum Sonenberg,[3] and Antonis E. Koromilas[1]*

Lady Davis Institute for Medical Research[1] and Department of Biochemistry,[3] McGill University, Montreal, Quebec, and Ottawa Regional Cancer Centre Research Laboratories, Ottawa, Ontario,[2] Canada

Received 20 February 2004/Accepted 26 July 2004

Phosphorylation of the alpha (α) subunit of the eukaryotic translation initiation factor 2 (eIF2) leads to the inhibition of protein synthesis in response to diverse stress conditions, including viral infection. The eIF2α kinase PKR has been shown to play an essential role against vesicular stomatitis virus (VSV) infection. We demonstrate here that another eIF2α kinase, the endoplasmic reticulum-resident protein kinase PERK, contributes to cellular resistance to VSV infection. We demonstrate that mouse embryonic fibroblasts (MEFs) from PERK$^{-/-}$ mice are more susceptible to VSV-mediated apoptosis than PERK$^{+/+}$ MEFs. The higher replication capacity of VSV in PERK$^{-/-}$ MEFs results from their inability to attenuate viral protein synthesis due to an impaired eIF2α phosphorylation. We also show that VSV-infected PERK$^{-/-}$ MEFs are unable to fully activate PKR, suggesting a cross talk between the two eIF2α kinases in virus-infected cells. These findings further implicate PERK in virus infection, and provide evidence that the antiviral and antiapoptotic roles of PERK are mediated, at least in part, via the activation of PKR.

Various forms of stress, including virus infection, can lead to the inhibition of the overall rates of protein synthesis (9, 22). This translational control is mediated at the level of initiation mainly through the phosphorylation of the alpha (α) subunit of the eukaryotic translation initiation factor 2 (eIF2) (22). Phosphorylated eIF2α at serine 51 functions as a dominant inhibitor of the guanine exchange factor eIF2B and impedes recycling of eIF2 between successive rounds of protein synthesis (15). To date, four distinct eukaryotic eIF2α kinases have been identified; these are the heme-regulated inhibitor, also known as heme control repressor (5), the double-stranded RNA (dsRNA)-activated protein kinase PKR (22), the PKR-like endoplasmic reticulum (ER)-resident protein kinase PERK (or PEK) (31), and the homologue of the *Saccharomyces cerevisiae* protein kinase GCN2 (23). Functional characterization of these kinases has indicated that each enzyme controls mRNA translation in response to a specific type of stimuli (9). However, the existence of several related eIF2α specific kinases is likely to provide cells with a certain degree of redundancy of function (22).

PERK is a type I transmembrane protein, located in the ER, that possesses a lumenal domain able to recognize incorrectly folded proteins (13, 31). Accumulation of unfolded proteins in the ER induces a signaling cascade from the cytoplasmic kinase domain of PERK, leading to its autophosphorylation and induction of eIF2α phosphorylation, which in turn, downregulates the synthesis of incorrectly folded proteins (13). The kinase plays an essential role in the ER-mediated cellular response known as the unfolded protein response (UPR), protecting cells from a protein overloaded ER by shutting down the translational machinery (13).

Among the eIF2α kinases, PKR has been clearly implicated in virus infection (22). The kinase is expressed at low levels in all normal tissues but is transcriptionally induced by type I interferons (i.e., alpha/beta interferon [IFN-α/β]), which are secreted by the host tissue in response to virus infection (36). Binding of PKR to dsRNA produced during virus replication induces conformational alterations that facilitate dimerization and autophosphorylation of the kinase on multiple serine and threonine residues, modifications that render it active (22). Active PKR then phosphorylates eIF2α at the ribosomal interface, which in turn leads to a general inhibition of protein synthesis and blockade of viral replication. The kinase has been shown to be required for host resistance to a variety of viruses (21). For example, it has been shown that PKR$^{-/-}$ mice are highly susceptible to intranasal vesicular stomatitis virus (VSV) infection, and the kinase is a major component of IFN-mediated resistance to VSV infection (2, 11, 37). However, unlike the mice, PKR$^{-/-}$ mouse embryonic fibroblasts (MEFs) are modestly more permissive to VSV replication (11, 37), indicating that the lack of PKR might be compensated for by the expression of another eIF2α kinase, whose activity is induced by VSV infection.

Although PKR is primarily involved in translation inhibition in virus-infected cells, recent findings have implicated PERK in hepatitis C virus replication (27). We demonstrate here the antiviral and antiapoptotic roles of PERK in VSV infection. We show that PERK$^{-/-}$ MEFs are highly susceptible to VSV-mediated induction of apoptosis as a result of higher virus replication caused by the inability of cells to fully induce eIF2α phosphorylation. We further show that VSV infection does not

* Corresponding author. Mailing address: Lady Davis Institute for Medical Research, Jewish General Hospital, 3755 Côte-Ste-Catherine St., Montreal, Quebec H3T 1E2, Canada. Phone: (514) 340-8260, ext. 3697. Fax: (514) 340-7576. E-mail: antonis.koromilas@mcgill.ca.

elicit an ER stress response but rather requires the activation of PKR, which occurs downstream of PERK. Our findings provide evidence, for the first time, that a cross talk between PKR and PERK is necessary for host resistance to VSV infection.

MATERIALS AND METHODS

Tissue culture and transfections. $PERK^{+/+}$ and $PERK^{-/-}$ MEF, HeLa, Vero, and COS-1 cells were maintained in Dulbecco modified Eagle medium (DMEM; Gibco) supplemented with 10% heat-inactivated calf serum and antibiotics (penicillin-streptomycin, 100 U/ml; ICN Biomedicals, Inc.). Cells were treated with IFN-α/β (1,000 IU/ml), IFN-γ (100 IU/ml), thapsigargin (TG; 1 μM), tunicamycin (10 μg/ml), and zVAD-fmk (10 μM) or infected with VSV (Indiana serotype) at the multiplicities of infection (MOI) indicated in the figures. For transfection, 5×10^5 COS-1 cells were seeded in 6-cm plates and, the following day, cells were incubated with Lipofectamine Plus reagents (Invitrogen) and 5 μg of pcDNA plasmid containing wild-type PERK (WT-PERK), mutant PERK K618A (14), WT PKR, or dominant-negative PKRΔ6 (2 or 5 μg) (10). Cells were incubated in serum-free medium at 37°C for 5 h, followed by the addition of complete medium and incubation for an additional 36 h before being infected with VSV (MOI 10, 12 h) or treated with TG (1 μM, 2 h). Protein extraction was prepared as described below.

Protein extraction and Western blot analysis. Cells were washed twice with ice-cold phosphate-buffered saline, and proteins were extracted in ice-cold lysis buffer containing 10 mM Tris-HCl (pH 7.5), 50 mM KCl, 2 mM $MgCl_2$, 1% Triton X-100, 3 μg of aprotinin/ml, 1 μg of pepstatin/ml, 1 μg of leupeptin/ml, 1 mM dithiothreitol (DTT), 0.1 mM Na_3VO_4, and 1 mM phenylmethylsulfonyl fluoride. Extracts were kept on ice for 15 min and centrifuged at $10,000 \times g$ for 15 min (4°C), and supernatants were stored at −80°C.

Protein extracts (50 μg) were subjected to sodium dodecyl sulfate-polyacrylamide gel electrophoresis (SDS-PAGE) as described previously (32). Proteins were then electroblotted onto polyvinylidene difluoride membranes (Immobilon P; Millipore), which were incubated with any of the following primary antibodies (at a 1:1,000 dilution): goat polyclonal antibody to PERK (T-19; Santa Cruz), rabbit polyclonal antibody to phosphothreonine 980 of PERK (Cell Signaling), rabbit polyclonal antibody to PERK (H-300; Santa Cruz), rabbit polyclonal antibody to phosphoserine 51 of eIF-2α (BioSource), mouse monoclonal antibody to eIF2α (3), rabbit polyclonal antibody to caspase-12 (Cell Signaling), mouse monoclonal antibody to Myc epitope (9E10; Santa Cruz), rabbit polyclonal antibody to phospho-JNK-1 (Cell Signaling), rabbit polyclonal antibody to JNK-1 (Cell Signaling), rabbit polyclonal antibody to phospho-p38 mitogen-activated protein kinase (MAPK; Cell Signaling), rabbit polyclonal antibody to p38 MAPK (Cell Signaling), mouse monoclonal antibody to PKR (B-10; Santa Cruz), rabbit polyclonal antibody to PKR (D-20; Santa Cruz), rabbit polyclonal antibody to phosphothreonine446 PKR (UBI), rabbit polyclonal antibody to VSV (1:5,000 dilution; manufactured by Earl Brown), rabbit polyclonal antibody to PARP (Cell Signaling), mouse monoclonal antibody to Actin (1:5,000 dilution; Clone C4, ICN Biomedicals, Inc.). Anti-mouse immunoglobulin G (IgG)-horseradish peroxidase (HRP)-, anti-goat IgG-HRP-, or anti-rabbit IgG-HRP-conjugated antibodies were used as secondary antibodies (1:1,000 dilution). Proteins were visualized by enhanced chemiluminescence according to manufacturer's specification (Amersham Life Sciences, Inc.).

Flow cytometry analysis. Apoptotic assays were carried out by surface staining with the annexin V fluorescein isothiocyanate apoptosis kit (BioSource) according to the manufacturer's instructions. The stained cells were analyzed by flow cytometry using a FACScan (Becton Dickinson), and data were analyzed by using WinMDI version 2.8 software (The Scripps Institute). Samples were gated on a dot plot showing forward scatter and side scatter in order to exclude cell debris not within normal cell size. Gated cells were plotted on a dot-plot showing annexin V staining (FL1-H) and propidium iodide (PI) staining (FL2-H).

Two-dimensional (2D) gel electrophoresis. $PERK^{+/+}$ and $PERK^{-/-}$ MEFs were infected with VSV or treated with TG before being lysed with 8 M urea, 4% (wt/vol) CHAPS {3-[(3-cholamidopropyl)-dimethylammonio]-1-propanesulfonate}, 65 mM DTT, and 0.5% (vol/vol) IPG buffer (pH 4 to 7 or pH 6 to 11) (Bio-Rad). Isoelectric focusing (IEF) step was performed by using an Ettan IPGphor IEF unit (Amersham) and 7-cm strips at pH 4 to 7 or pH 6 to 11 (Bio-Rad). The strips were passively rehydrated with 125 μl of rehydration buffer containing 80 μg of the protein extracts, 8 M urea, 2% (wt/vol) CHAPS, 10 mM DTT, 0.5% (vol/vol) IPG buffer (pH 4 to 7 or pH 6 to 11), and a trace amount of bromophenol blue for 10 h. IEF was performed at 150 V for 40 min, 500 V for 40 min, 1,000 V for 40 min, and 5,000 V for 2.5 h. The strips were then equilibrated for 12 min in 50 mM Tris-HCl (pH 8.8), 6 M urea, 30% glycerol, 2% SDS, 1% (wt/vol) DTT, and a trace amount of bromophenol blue. The strips were then incubated for 5 min in 50 mM Tris-HCl (pH 8.8), 6 M urea, 30% glycerol, 2% SDS, 2.5% (wt/vol) iodoacetamide, and a trace amount of bromophenol blue. The equilibrated strips were then subjected to second-dimension analysis with SDS–10% PAGE, followed by immunoblot analysis.

PKR autophosphorylation assay. $PERK^{+/+}$ and $PERK^{-/-}$ MEFs were either infected with VSV (MOI = 10) or treated with tunicamycin (10 μg/ml) or dsRNA (10 μg/ml). Cells were treated for the indicated periods of time. Proteins were extracted in the ice-cold lysis buffer described above. Whole-cell extracts (130 to 200 μg of protein) were used for a pulldown assay with poly(rI-rC) dsRNA coupled to agarose beads (type 6; Amersham Biosciences) or for an immunoprecipitation with the anti-mPKR antibody (D-20). The bound proteins were equilibrated in a previously described kinase buffer (3) and then incubated in the presence of 1 μCi of [γ-^{32}P]ATP. The reactions were incubated at 30°C for 30 min and subjected to SDS–10% PAGE, followed by either immunoblot analysis with the anti-mPKR antibody (B-10) or autoradiography.

VSV plaque assay. The VSV plaque assay protocol was previously described (33). Briefly, $PERK^{+/+}$ and $PERK^{-/-}$ MEFs were infected with VSV (MOI = 1 or 100). At 1 h postinfection (hpi), the nonadherent virus was removed and plates were washed twice with serum-free DMEM and replenished with complete medium. At different times postinfection, the medium was collected, diluted with serum-free DMEM, and then used to infect Vero cells (100% confluence). At 1 hpi, medium from the Vero cells was removed and replaced with complete medium containing 0.5% methyl cellulose (Sigma-Aldrich) for 24 to 36 h. Vero cells were fixed in 4% formaldehyde and stained with crystal violet. Plaques were counted, and titers were calculated as PFU per milliliter. Triplicate experiments were performed, and the averages of the virus titers were calculated.

RESULTS

Susceptibility of $PERK^{-/-}$ MEFs to VSV-mediated apoptosis. We sought to determine whether PERK plays a role in VSV replication. To do so, we first assessed the susceptibility of $PERK^{+/+}$ and $PERK^{-/-}$ MEFs to VSV-mediated apoptosis. That is, we tested the viability of noninfected or VSV-infected (MOI = 1) MEFs at different times postinfection (Fig. 1A). We noticed that a higher number of $PERK^{-/-}$ than $PERK^{+/+}$ MEFs were susceptible to the cytopathic effects of VSV (Fig. 1A). Pretreatment with IFN-α/β completely protected both $PERK^{+/+}$ and $PERK^{-/-}$ MEFs against VSV infection (Fig. 1B). To establish whether $PERK^{-/-}$ MEFs were indeed undergoing apoptosis, $PERK^{+/+}$ and $PERK^{-/-}$ MEFs infected with VSV were analyzed for staining with annexin V, an indicator of early apoptosis (Fig. 2A and B). We found that at 24 hpi almost 30% of $PERK^{-/-}$ MEFs were apoptotic compared to 10% of the $PERK^{+/+}$ MEFs, whereas at 36 hpi the population of apoptotic $PERK^{-/-}$ MEFs reached 60% compared to 20% of the $PERK^{+/+}$ MEFs (Fig. 2A and B). We also examined whether the increased susceptibility of $PERK^{-/-}$ MEFs to VSV infection is affected by treatment with either IFN-α/β (Fig. 2A and B, middle rows) or IFN-γ (Fig. 2A and B, bottom rows). Pretreatment with either type of IFN eliminated the apoptotic effects of VSV infection in both $PERK^{+/+}$ and $PERK^{-/-}$ MEFs, indicating that IFN signaling remains intact in $PERK^{-/-}$ MEFs and that expression of one or more IFN-induced genes can compensate for the loss of PERK in these cells.

We then performed viral plaque assays in order to determine whether the susceptibility of $PERK^{-/-}$ MEFs to VSV infection was due to a higher virus production. We determined that VSV production increased exponentially in $PERK^{-/-}$ MEFs (MOI = 1; Fig. 2C, left panel) with a 3-log-higher titer than $PERK^{+/+}$ MEFs at 12 hpi and a 4- or 8-log-higher titer at

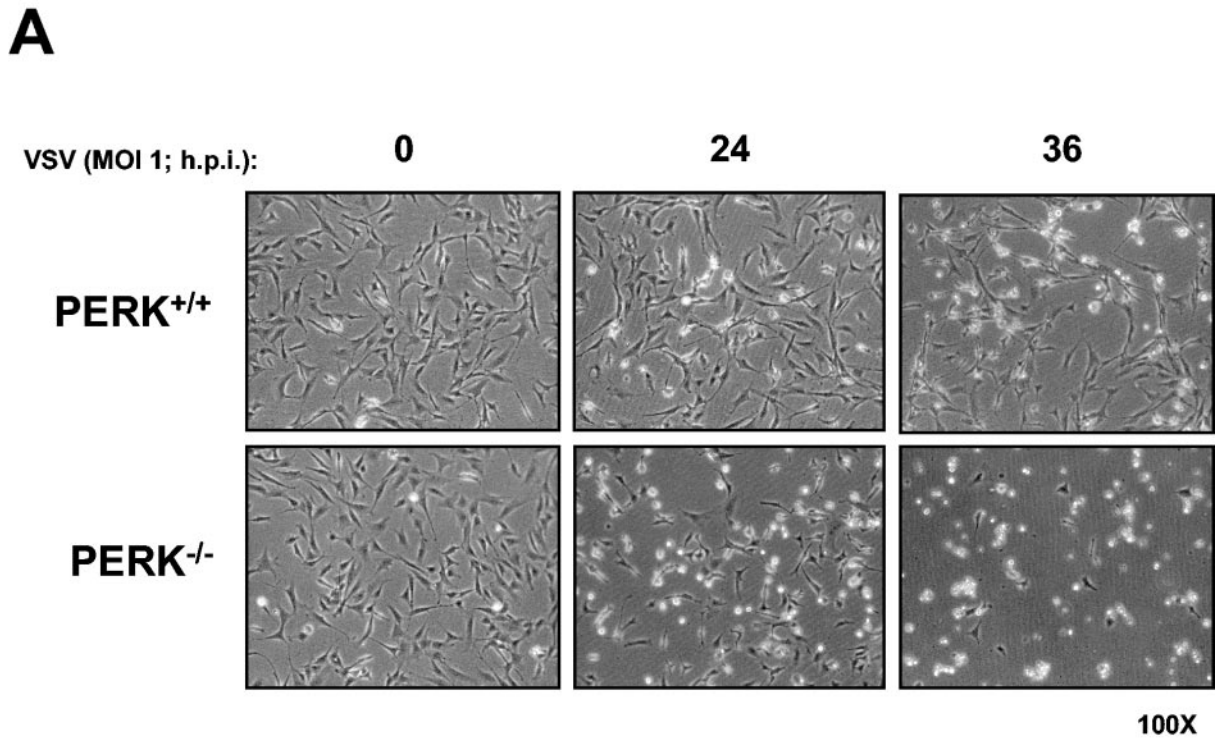

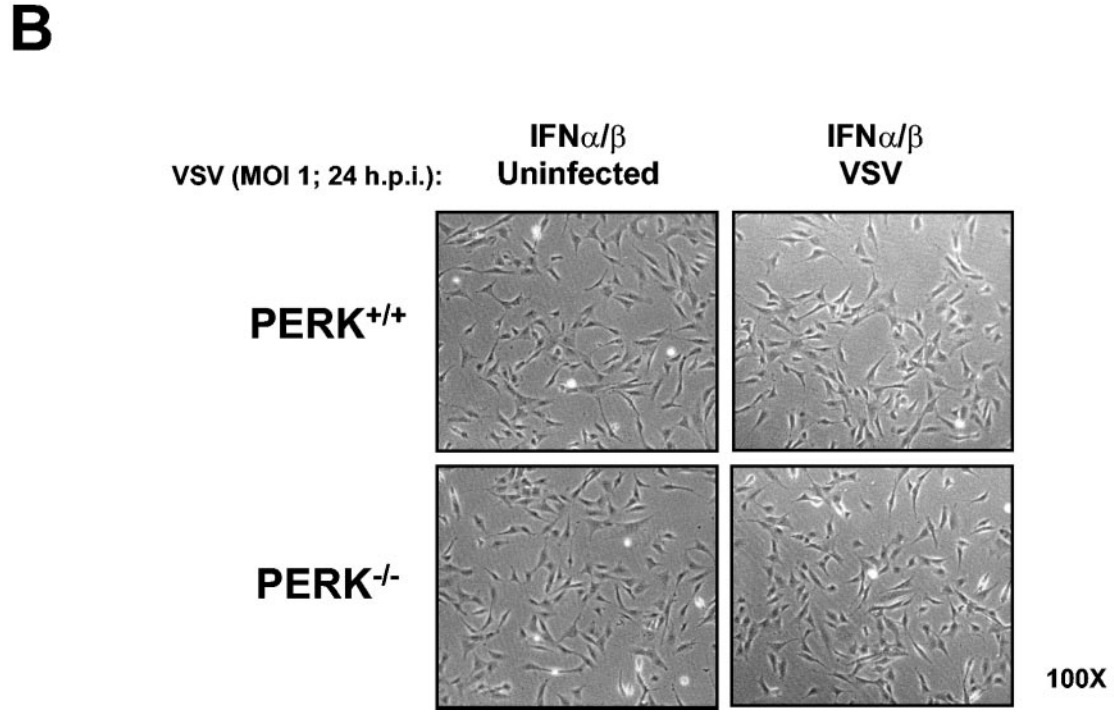

FIG. 1. Increased susceptibility of PERK$^{-/-}$ MEFs to VSV infection. PERK$^{+/+}$ and PERK$^{-/-}$ MEFs were left untreated (A) or treated with mouse IFN-α/β (1,000 IU/ml) (B) for 18 h in the absence (A and B, left panels) or presence (A and B, right panels) of VSV infection at an MOI of 1. Cells were photographed at ×100 magnification at indicated times postinfection.

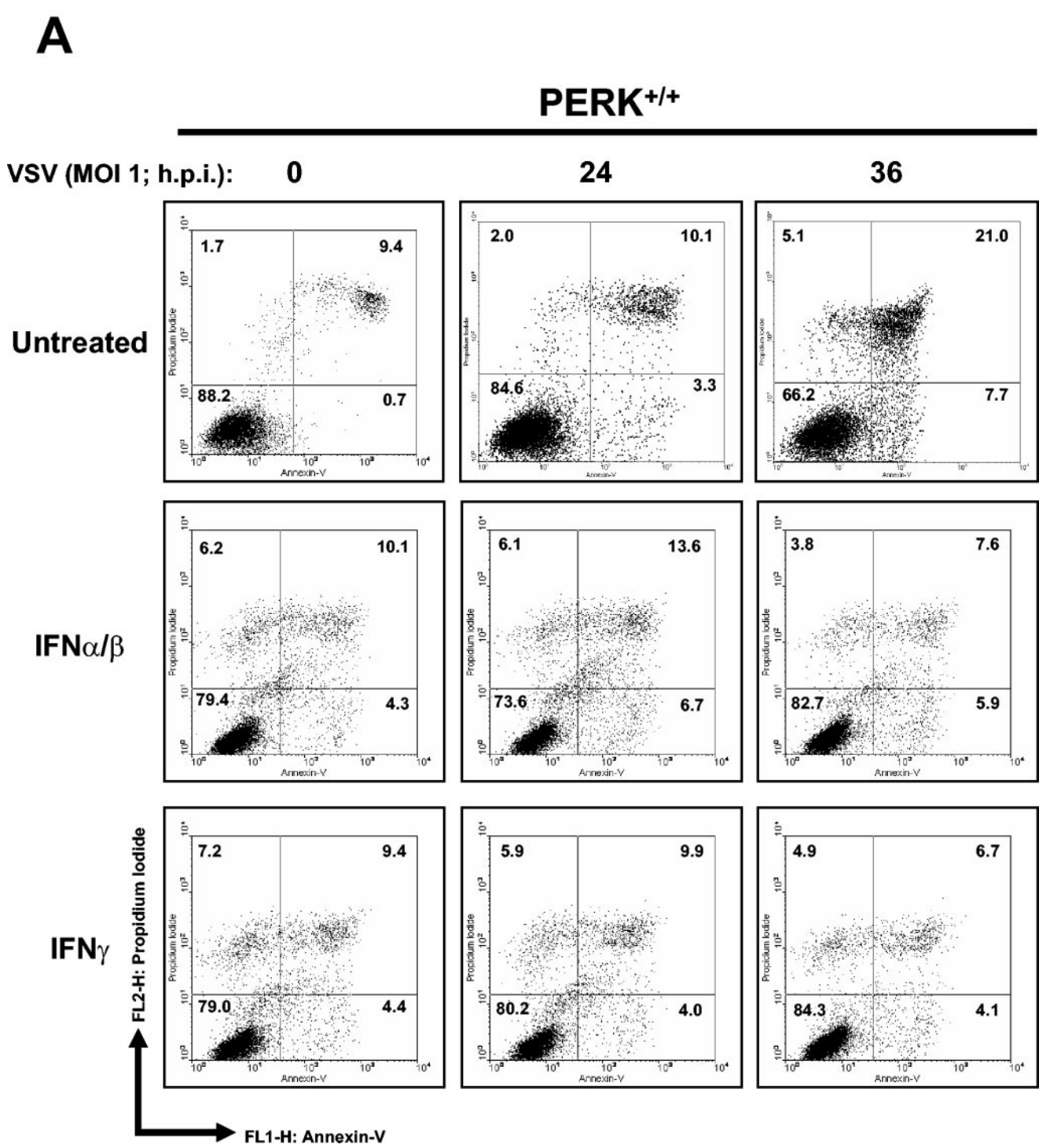

FIG. 2. Higher induction of VSV-mediated apoptosis in PERK$^{-/-}$ MEFs. PERK$^{+/+}$ (A) and PERK$^{-/-}$ (B) MEFs were left untreated or treated with either mouse IFN-α/β (1,000 IU/ml) or IFN-γ (100 IU/ml) for 20 h, followed by infection with VSV at an MOI of 1. Cells were harvested at 24 or 36 hpi and subjected to annexin V-PI staining (BioSource) according to the manufacturer's specifications. Cells were then subjected to flow cytometry analysis by using FACScan (Becton Dickinson), and data were analyzed by using WinMDI version 2.8 software (The Scripps Institute). Cells were gated on a dot plot showing forward and side scatter in order to exclude debris not within the normal size. Gated cells were plotted on a dot plot showing annexin V staining (FL1-H) and PI straining (FL2-H). The numbers represent the percentage of gated cells counted for their corresponding quadrant. These are data of one out of three reproducible experiments. (C and D) PERK$^{+/+}$ and PERK$^{-/-}$ MEFs were left uninfected or were infected with VSV at an MOI of 1 (C) or an MOI of 100 (D); protein extracts (30 μg) were subjected to immunoblot analysis with an anti-VSV antibody (right panels), or virus titers were measured by harvesting medium at the indicated times postinfection, followed by plaque assay analysis (left panels). Symbols: ▲, virus titers from PERK$^{+/+}$ MEFs; ■, virus titers from PERK$^{-/-}$ MEFs.

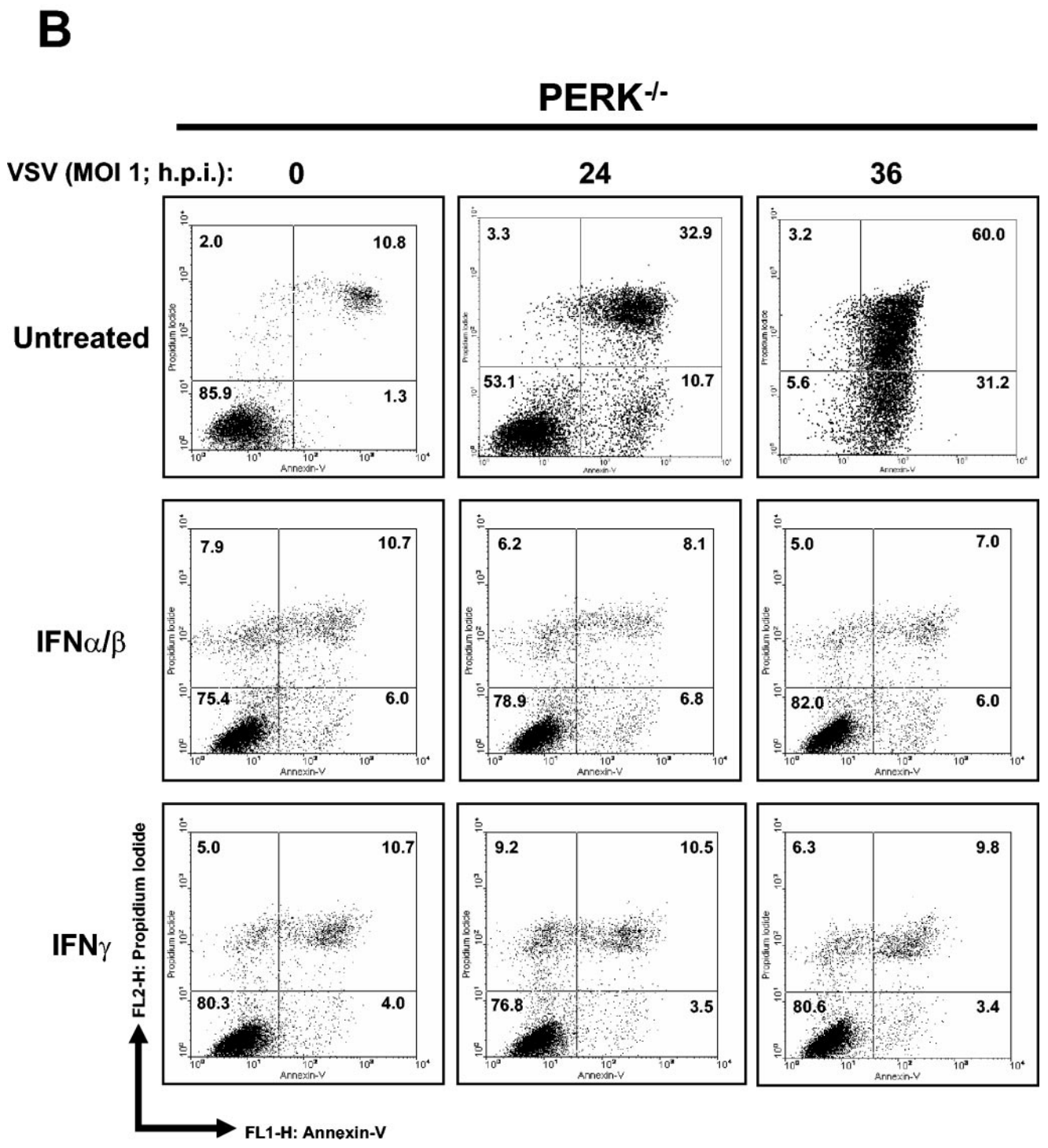

FIG. 2—*Continued*.

24 or 36 hpi, respectively. Immunoblot analysis with an anti-VSV antibody revealed that VSV protein production was only detectable in PERK$^{-/-}$ MEFs infected at an MOI of 1 (Fig. 2C, right panel). Despite the fact that the VSV titer increased in PERK$^{+/+}$ MEFs infected at an MOI of 100 (Fig. 2D, left panel), it remains relatively lower than in PERK$^{-/-}$ MEFs (twofold lower at 4 hpi) throughout the growth curve, and virus production reached a plateau after 8 hpi. The right panel of Fig. 2D clearly shows that VSV replication was significantly higher in infected PERK$^{-/-}$ MEFs due to robust viral protein production. These results explain that the susceptibility of PERK$^{-/-}$ MEFs to VSV-mediated apoptosis is due to higher viral protein production and the release of progeny virions.

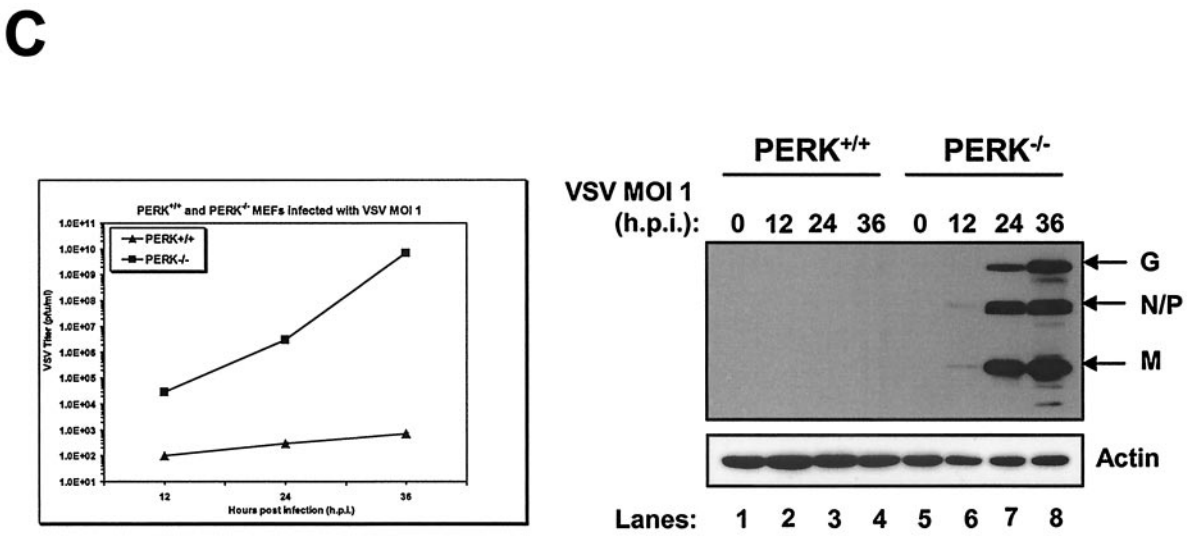

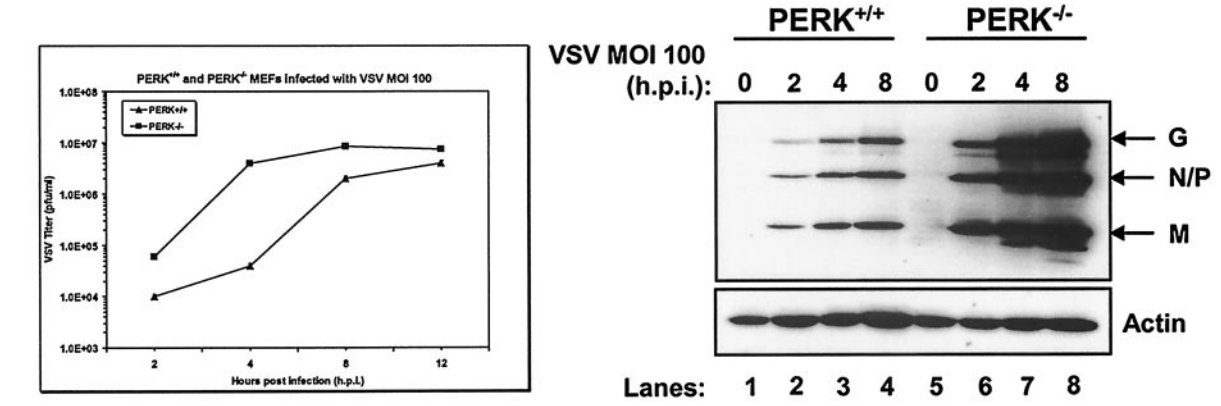

FIG. 2—*Continued*.

Impaired eIF2α phosphorylation in VSV-infected PERK$^{-/-}$ MEFs. To further characterize the PERK$^{-/-}$ MEFs, we next evaluated the eIF2α phosphorylation levels in response to VSV infection at different MOIs (1, 10, and 50). We reasoned that VSV replication might activate intracellular pathways, leading to PERK-mediated eIF2α phosphorylation. VSV infection induced eIF2α phosphorylation levels in both types of MEFs; however, eIF2α phosphorylation was induced at higher levels in PERK$^{+/+}$ MEFs than in PERK$^{-/-}$ MEFs (Fig. 3A to C, top panels). To further verify this observation, we measured the eIF2α phosphorylation levels in VSV-infected MEFs by using 2D gel electrophoresis (Fig. 3D). We noticed that phosphorylation of eIF2α was increased in PERK$^{+/+}$ MEFs versus PERK$^{-/-}$ MEFs after infection with VSV or treatment with the ER stress inducer TG (compare the top panels with the middle or bottom panels). These data suggested that the higher levels of eIF2α phosphorylation can limit VSV replication in PERK$^{+/+}$ MEFs as opposed to PERK$^{-/-}$ MEFs, in which eIF2α phosphorylation was diminished.

VSV induces PERK-mediated eIF2α phosphorylation in transiently transfected cells. Next, we performed immunoblot analysis with a phospho-specific antibody against the Thr980 phosphorylation site of PERK, a site that serves as a marker for activation, by using VSV-infected HeLa cells to detect endogenous PERK phosphorylation (Fig. 4A). PERK phosphorylation was induced as early as 2 hpi. TG treatment for 1 h was used as a positive control. A shift in PERK migration was observed in TG-treated cells as opposed to VSV-infected cells,

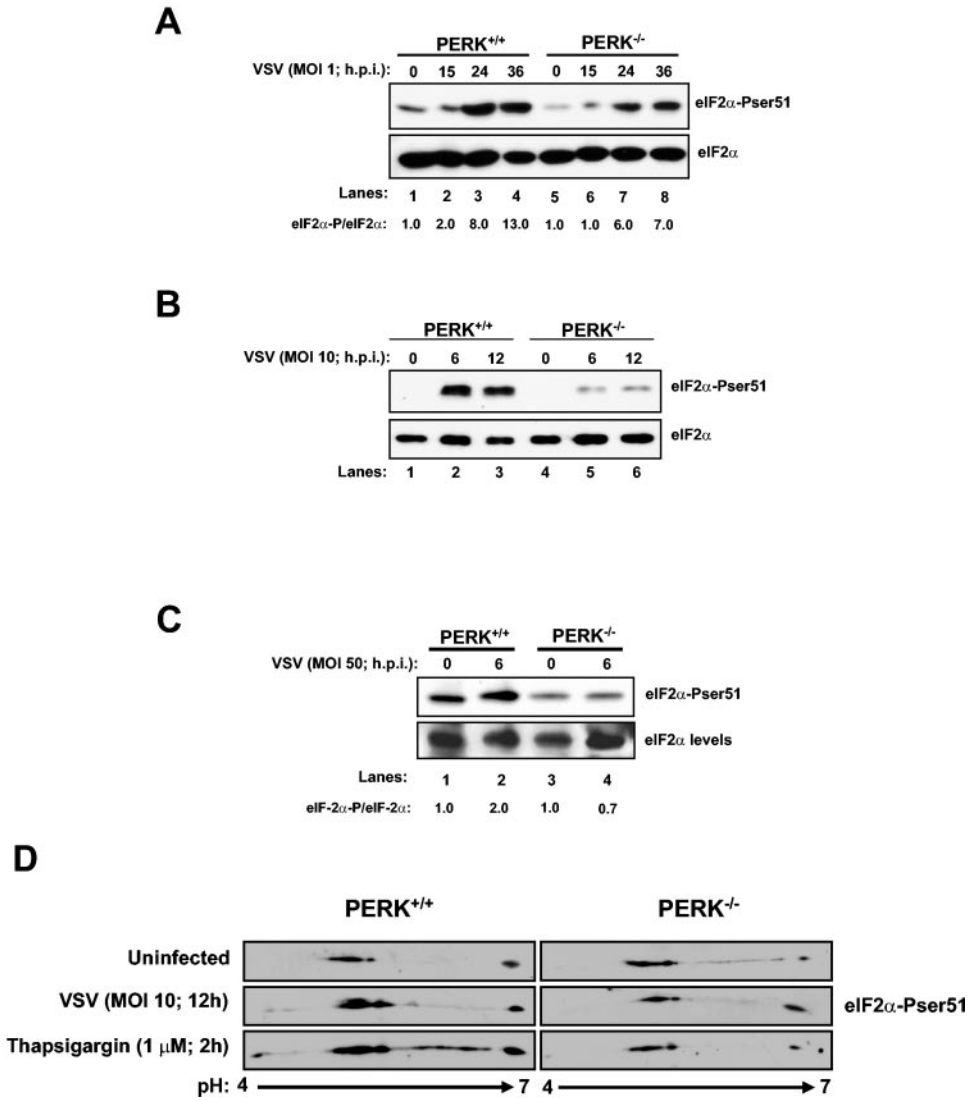

FIG. 3. Enhanced VSV replication in PERK$^{-/-}$ MEFs as a result of impaired eIF2α phosphorylation. PERK$^{+/+}$ and PERK$^{-/-}$ MEFs were infected (lanes 2 to 4 and lanes 6 to 8) or not infected (lanes 1 and 5) with VSV at MOIs of 1 (A), 10 (B), or 50 (C). Protein extracts were harvested at the indicated times postinfection and subjected to immunoblot analysis by using the rabbit polyclonal anti-phosphoserine 51 eIF2α antibody (top panels) or with the eIF2α panspecific antibody (lower panels). The ratio of phosphorylated to total eIF2α protein for each lane is indicated. (D) PERK$^{+/+}$ and PERK$^{-/-}$ MEFs were treated with 1 μM TG for 2 h (bottom panels), infected (middle panels) or not infected (top panels) with VSV at an MOI of 10, and harvested at 12 hpi. Protein extracts (80 μg) were subjected to 2D electrophoresis and immunoblot analysis with a rabbit polyclonal anti-phosphoserine 51 eIF2α antibody.

indicating that TG induces a higher phosphorylation pattern of PERK than VSV infection.

To further substantiate the above findings, we performed transient transfections of plasmids that express either WT-PERK or the kinase-inactive mouse PERK bearing the K618A mutation in COS-1 cells (Fig. 4B). We reasoned that if PERK is activated by VSV infection, then eIF2α phosphorylation should be induced in cells transfected with the WT kinase as opposed to cells expressing the catalytically inactive kinase. The expression of both proteins was detected by immunoblotting with either an anti-Myc tag antibody (second panel) or with an anti-PERK antibody (third panel). In the absence of VSV infection, we noticed that WT-PERK migrated more slowly than PERK K618A due to the autophosphorylation of the active kinase (Fig. 4, lanes 2 and 3, second and third panels) (14).

On the other hand, we noticed in VSV-infected cells infected a slight shift in the mobility of WT-PERK after immunoblotting with both antibodies (second and third panels, compare lanes 2 and 5), indicating PERK activation during virus replication. Activation of PERK became more evident after immunoblotting with the phosphothreonine 980 antibody (top panel). We detected an induction in PERK phosphorylation upon VSV infection (lane 5, top panel) and in cells treated with TG (lane 8, top panel) compared to uninfected or untreated cells (lane 2, top panel). As expected, this phospho-specific antibody was unable to detect the PERK K618A mu-

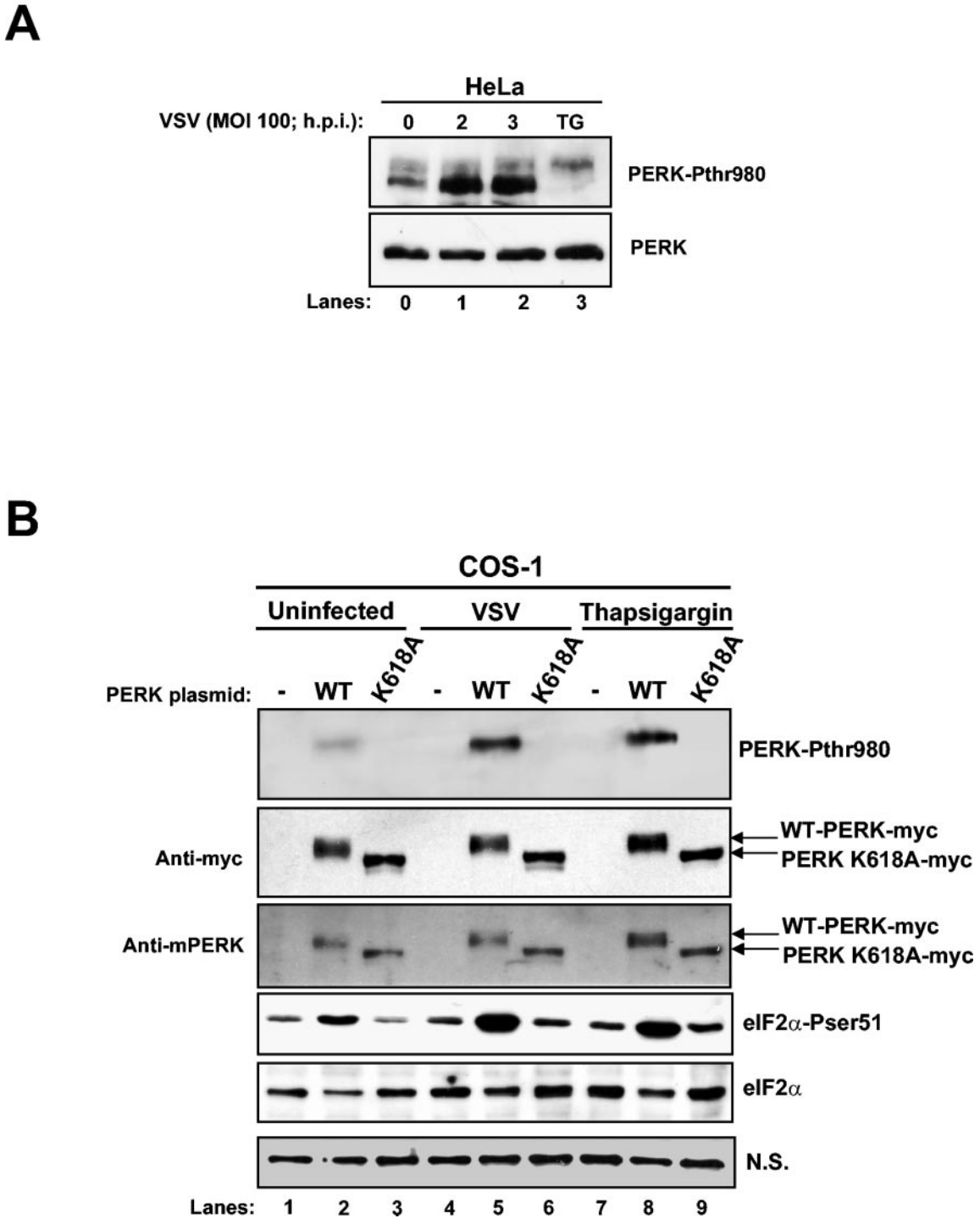

FIG. 4. VSV induces PERK-mediated eIF2α phosphorylation. (A) Protein extracts from HeLa cells infected with VSV (MOI = 100) were collected at different times postinfection and subjected to immunoblot analysis with a rabbit polyclonal phosphothreonine 980 PERK antibody (top panel) or a rabbit polyclonal anti-PERK antibody (H-300; bottom panel). (B) COS-1 cells were transfected with either Myc-tagged WT-PERK or the K618A catalytic mutant of mouse PERK (5 μg of plasmid DNA), followed by VSV infection or TG treatment. Protein extracts were subjected to immunoblot analysis with a rabbit polyclonal phosphothreonine 980 PERK antibody (top panel), a mouse monoclonal Myc-tag antibody (second panel), a goat polyclonal anti-PERK antibody (third panel), a rabbit polyclonal phosphoserine 51 eIF2α antibody (fourth panel), or a mouse monoclonal eIF2α panspecific antibody (fifth panel). A nonspecific (N.S.) band was used to determine the amount of protein loaded (bottom panel).

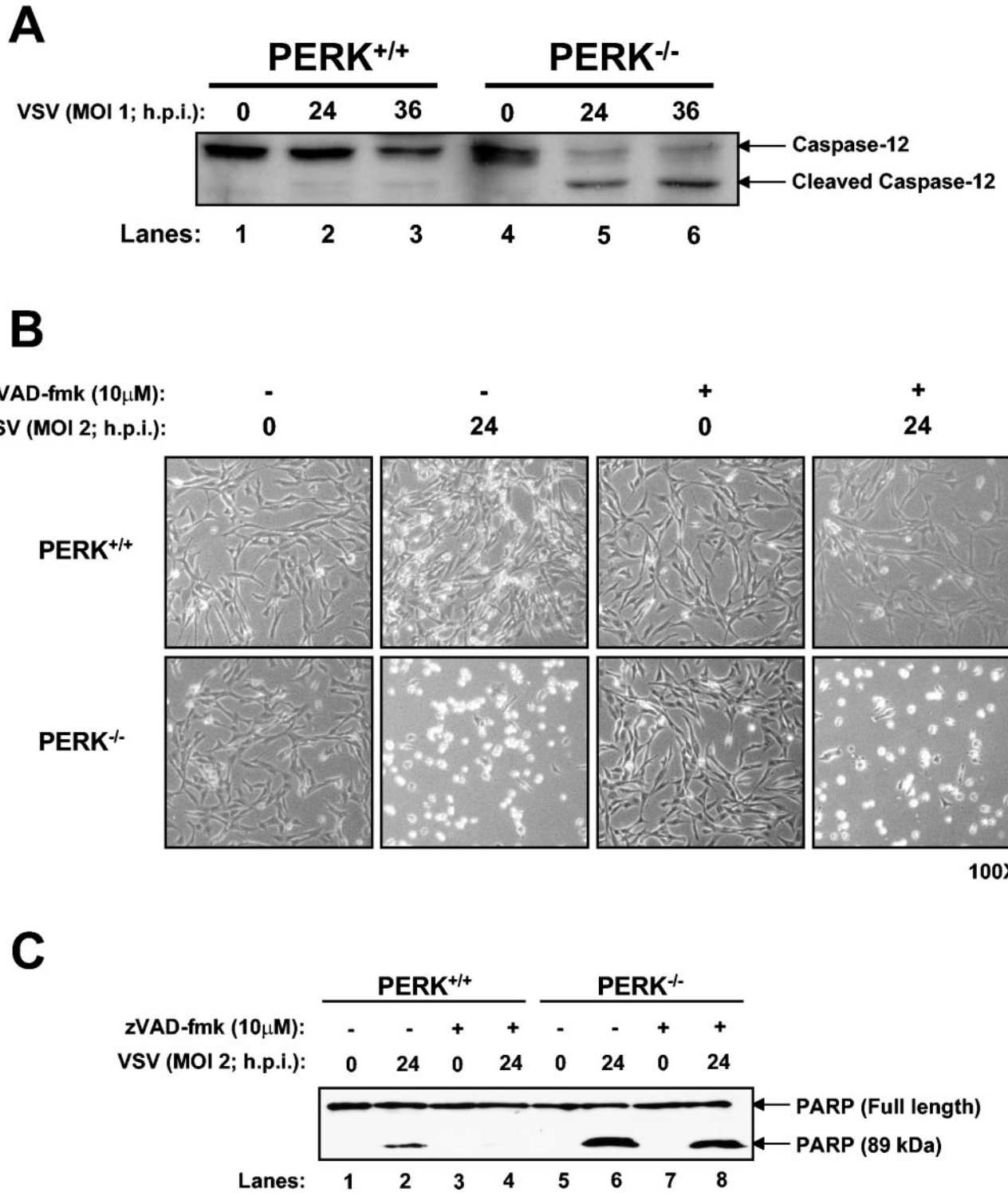

FIG. 5. VSV-induced apoptosis of PERK$^{-/-}$ MEFs proceeds through caspase-12 activation. (A) Protein extracts from PERK$^{+/+}$ and PERK$^{-/-}$ MEFs infected with VSV (MOI = 1) were collected at different times postinfection and subjected to immunoblot analysis with a rabbit polyclonal antibody to caspase-12. The upper band represents the inactive protease, whereas the lower band represents the cleaved and active enzyme. (B and C) PERK$^{+/+}$ and PERK$^{-/-}$ MEFs were either left untreated or treated with caspase inhibitors (zVAD-fmk; 10 μM) 2 h before infection with VSV (MOI = 2) for 24 h. Cells were photographed at ×100 magnification (B), or protein extracts (25 μg) were subjected to immunoblot analysis with a rabbit polyclonal antibody to PARP (C). The upper band represents the full-length 116-kDa PARP protein, and the lower band represents the cleaved 89-kDa PARP.

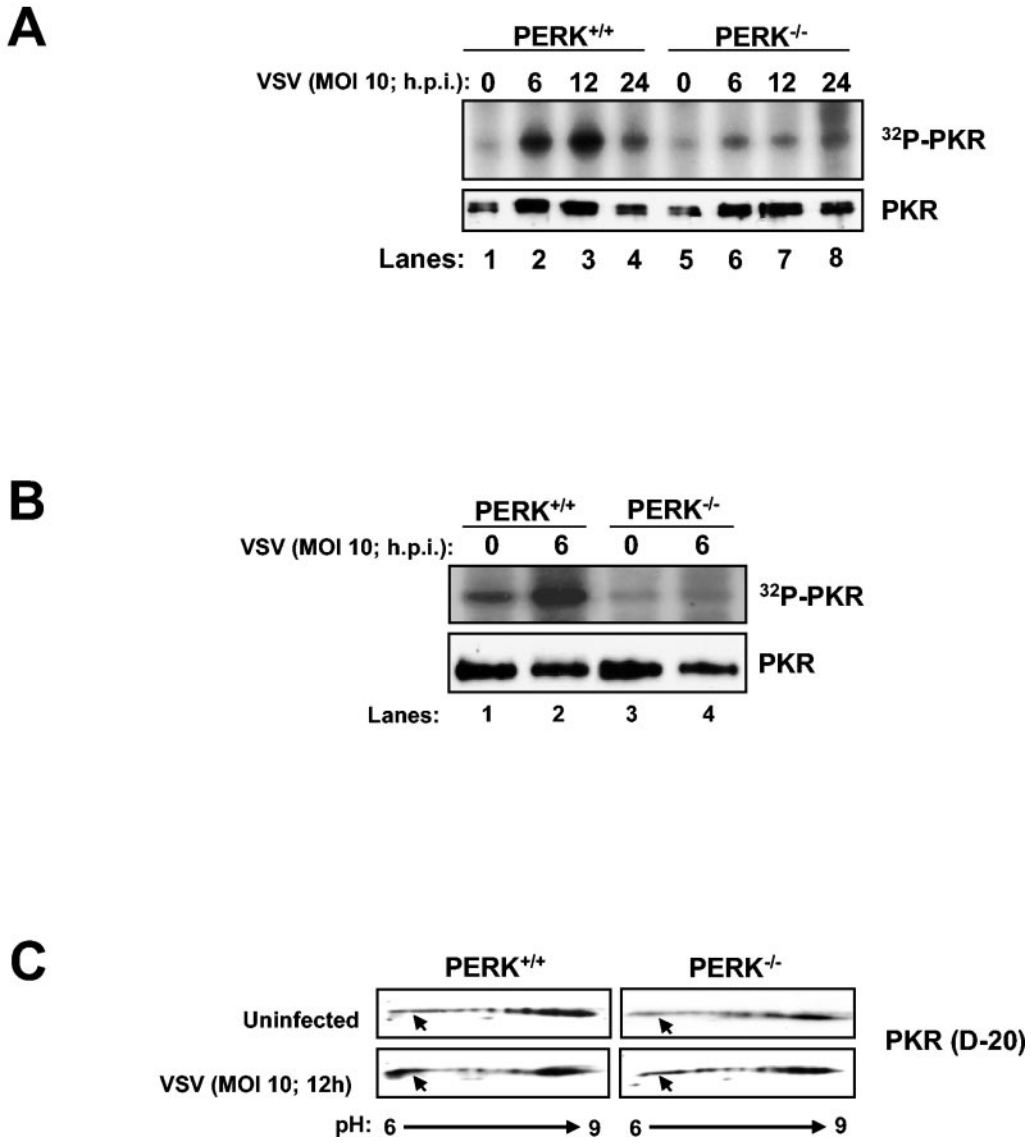

FIG. 6. PKR activation is impaired in VSV-infected PERK$^{-/-}$ MEFs. Protein extracts (130 μg) from VSV-infected (MOI = 10) PERK$^{+/+}$ and PERK$^{-/-}$ MEFs were either pulled down with poly(rI-rC)-agarose beads (Amersham-Pharmacia) (A) or immunoprecipitated with a rabbit polyclonal anti-mPKR antibody (D-20) (B) and then subjected to in vitro phosphorylation in the presence of [γ-^{32}P]ATP. Half of the dsRNA-bound PKR was subjected to SDS–10% PAGE and autoradiography (top panel), whereas the other half was subjected to immunoblot analysis with an antibody to mouse PKR (bottom panel, B-10). (C) PERK$^{+/+}$ and PERK$^{-/-}$ MEFs were either infected (bottom panels) or not infected (top panels) with VSV at an MOI of 10 and then harvested at 12 hpi. Protein extracts (80 μg) were subjected to 2D electrophoresis and immunoblot analysis with a rabbit polyclonal anti-mPKR antibody (D-20). (D) PERK$^{+/+}$ and PERK$^{-/-}$ MEFs were either treated or not treated with 10 μg of tunicamycin/ml for the indicated period of time. Protein extracts (130 μg) were subjected to a similar kinase assay as in panel A. (E) COS-1 cells were mock transfected (lanes 1 and 8) or transfected with either WT-PERK (5 μg of plasmid DNA; lanes 2, 4, 5, 9, 11, and 12) or WT PKR with (5 μg of plasmid DNA; lanes 6, 7, 13, and 14) or without PKRΔ6 (2 μg of plasmid DNA, lanes 4 and 11 or 5 μg of plasmid DNA; lanes 3, 5, 7, 10, 12, and 14), followed by VSV infection. Protein extracts were subjected to immunoblot analysis with either with a rabbit polyclonal phosphothreonine 980 PERK antibody (top panel), a mouse monoclonal Myc-tag antibody (second panel), a rabbit polyclonal phosphoserine 51 eIF2α antibody (third panel), or a mouse monoclonal eIF2α panspecific antibody (bottom panel).

tant since the latter mutation renders the kinase inactive (lanes 3, 6, and 9, top panel).

The induction of phosphorylation and activation of PERK upon VSV infection correlated with the eIF2α phosphorylation pattern we observed (fourth panel). We noticed that VSV infection induced eIF2α phosphorylation in cells transfected with WT-PERK compared to cells transfected with PERK-K618A mutant (compare lanes 5 and 6). In addition, eIF2α phosphorylation was significantly increased in VSV-infected cells than in uninfected cells expressing WT-PERK (compare lanes 2 and 5). Activation of WT-PERK and induction of eIF2α phosphorylation in transiently transfected COS-1 cells was also observed after treatment with TG, which served as a positive control in these assays (lanes 7 to 9). Based on these results, we concluded that VSV infection results in the induction of PERK activity and eIF2α phosphorylation.

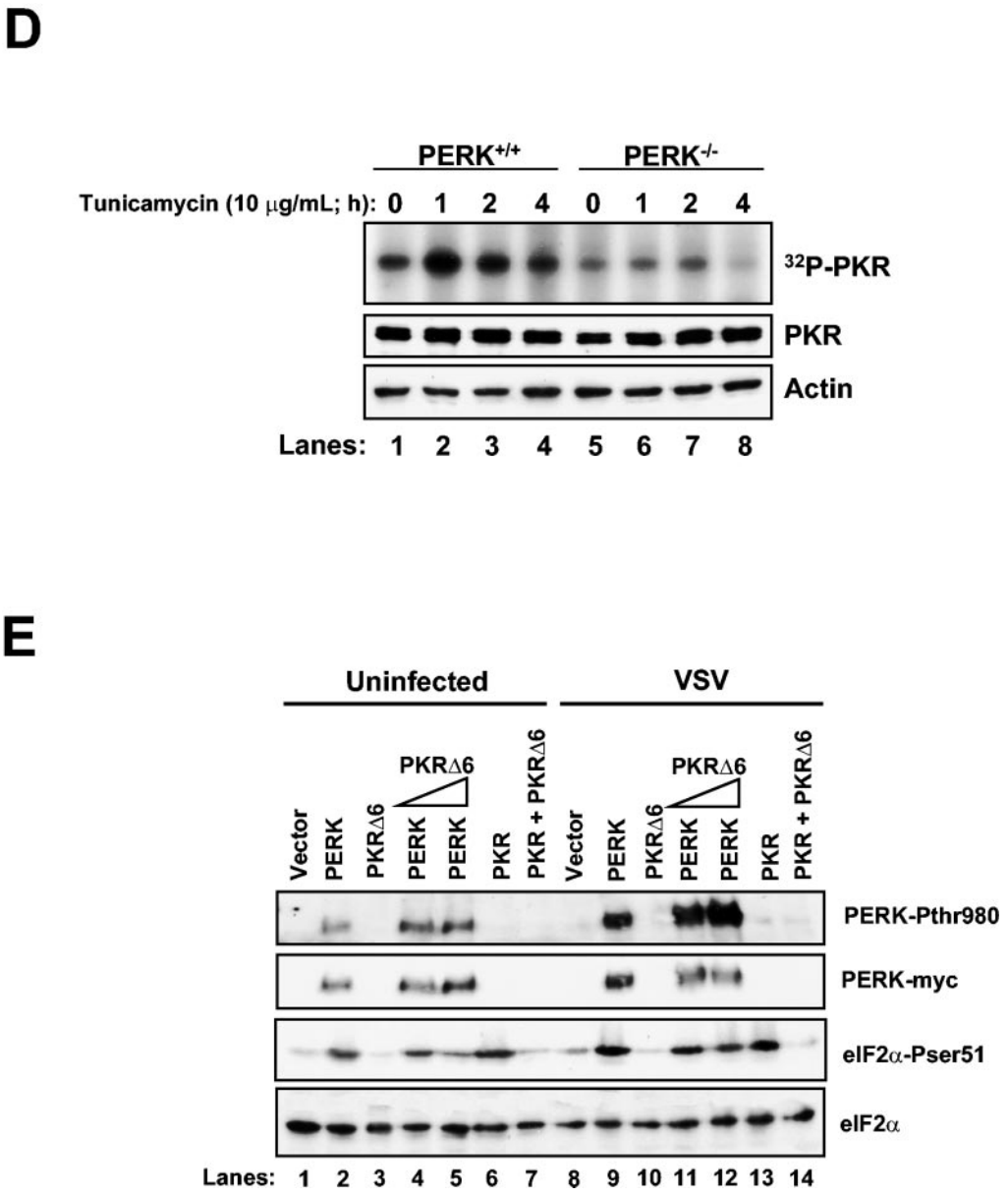

FIG. 6—*Continued*.

Caspase-12 induction in VSV-mediated apoptosis. In order to elucidate the mechanisms of VSV-mediated apoptosis, we measured caspase-12 activation in PERK$^{+/+}$ and PERK$^{-/-}$ MEFs in response to infection. Caspase-12 is an ER membrane-associated cysteine protease activated by ER stress (24). This protease is also induced in cells infected with the respiratory syncytial virus (4) or bovine viral diarrhea virus (19). Immunoblot analysis with an antibody that recognizes the inactive and active (i.e., cleaved) forms of caspase-12 demonstrated a higher activity of the protease in PERK$^{-/-}$ MEFs than in PERK$^{+/+}$ MEFs (Fig. 5A, compare lane 2 with lane 5 and lane 3 with lane 6). Thus, it appears that caspase-12 activation can account, at least in part, for the higher induction of VSV-mediated apoptosis in PERK$^{-/-}$ MEFs.

It was previously shown that broad-spectrum caspase inhibitors effectively prevented the activation of programmed cell death pathways in VSV-infected cells (7). In order to get a better understanding on VSV-mediated apoptosis, we treated PERK$^{+/+}$ and PERK$^{-/-}$ MEFs with a general caspase inhibitor (zVAD-fmk) prior to VSV infection. We noticed that caspase inhibitors protected PERK$^{+/+}$ from VSV infection (Fig. 5B, compare row 1, column 4, with row 1, column 2). However, the cell-rounding phenotype associated with VSV infection was not prevented in PERK$^{-/-}$ MEFs treated with caspase inhibitors (Fig. 5B, compare row 2, column 4, with row 2, column 2), indicating their inability to be rescued from VSV-mediated apoptosis.

This was further verified by immunoblot analysis of the poly(ADP ribose) polymerase (PARP), a common marker of apoptosis, where its cleavage is induced in VSV-infected cells (Fig.

5C) (16). VSV-infected PERK$^{-/-}$ MEFs had a higher PARP cleavage capacity than did PERK$^{+/+}$ cells (Fig. 5C, compare lane 6 with lane 2). When cells were treated with caspase inhibitors prior to VSV infection, PARP cleavage was abolished in PERK$^{+/+}$ cells, indicating apoptotic rescue (Fig. 5C, lane 4), whereas such inhibitors were unable to prevent PARP cleavage in PERK$^{-/-}$ MEFs (lane 8). This suggested that caspases play a critical role in VSV-mediated apoptosis in the presence of PERK. Conversely, in the absence of PERK, inactivation of caspases is not sufficient to abolish apoptosis, suggesting that the lack of PERK can induce caspase-independent apoptotic pathways.

ER-mediated apoptosis also proceeds through the activation of c-Jun NH_2-terminal kinase (JNK) (26). On the other hand, virus infection results in the activation of JNK-1 and p38 MAPK, both of which have been implicated in virus-mediated apoptosis (6, 18). Taken together, we sought to determine the expression and activity of these proapoptotic proteins in VSV-infected PERK$^{+/+}$ and PERK$^{-/-}$ MEFs. Immunoblot analysis with phospho-specific antibodies to either JNK-1 or p38 MAPK showed equal levels of expression and activation of these kinases in both types of MEFs (unpublished data). This indicated that the higher induction of VSV-mediated apoptosis in PERK$^{-/-}$ MEFs is independent of JNK-1 and p38 MAPK activation.

Cross talk between PERK and PKR during VSV replication. Given the demonstrated role for PKR in halting VSV replication (2, 11, 37), we wanted to examine whether induction of VSV replication and apoptosis in PERK$^{-/-}$ MEFs was due to defective activation of PKR. When protein extracts from VSV-infected cells were subjected to pulldown with poly(rI-rC)-agarose (Fig. 6A) or immunoprecipitation with PKR antibodies (Fig. 6B), followed by kinase autophosphorylation, we found that PKR kinase activity was severely diminished in PERK$^{-/-}$ MEFs as opposed to their WT counterparts after virus infection (Fig. 6A and B). This indicated that the higher replication and apoptotic capacity of VSV in PERK$^{-/-}$ MEFs is caused, at least in part, by defective PKR activation. We further verified this finding by assessing the activation of PKR in vivo by 2D gel electrophoresis and immunoblot analysis (Fig. 6C). We observed an increase in PKR protein toward the acidic side (pH 6; bottom left panel, arrow) in VSV-infected PERK$^{+/+}$ MEFs as opposed to the VSV-infected PERK$^{-/-}$ MEFs (bottom right panel). This acidic fraction of PKR was present only in PERK$^{+/+}$ cells, indicating an induction of PKR activity in cells containing PERK as opposed to cells lacking it.

This finding prompted us to examine whether PKR activity is induced by ER stress and, if so, whether its activation is mediated by PERK. To do so, we treated PERK$^{+/+}$ and PERK$^{-/-}$ MEFs with tunicamycin, an inhibitor of protein glycosylation and an ER stress inducer, followed by autophosphorylation of immunoprecipitated PKR (Fig. 6D). We noticed that PKR kinase activity was induced in PERK$^{+/+}$ MEFs upon tunicamycin treatment (lanes 1 to 4) as opposed to PERK$^{-/-}$ MEFs, which failed to activate PKR (lanes 5 to 8). Interestingly, PKR autophosphorylation was significantly diminished after 4 h of tunicamycin treatment (lane 8), indicating that prolonged ER stress may lead to the inactivation of PKR. These data provided evidence for a cross talk between the two eIF2α kinases with PKR functioning downstream of PERK in response to ER stress or VSV infection.

These data suggested that PERK can modulate PKR autophosphorylation and its full-scale activation. To further substantiate this, we cotransfected COS-1 cells with PERK or PKR in the presence or absence of a dominant-negative PKR mutant (PKRΔ6) (10) (Fig. 6E). PERK and PKR were able to induce eIF2α phosphorylation upon VSV infection (third panel, compare lanes 9 and 13 to lanes 2 and 6, respectively), whereas PKRΔ6 showed no kinase activity (third panel, compare lane 3 with lane 10). Also, PKRΔ6 was able to prevent PKR-mediated eIF2α phosphorylation before and after VSV infection (third panel, compare lane 7 with lane 14). To this extent, PKRΔ6 was capable of inhibiting PERK-mediated eIF2α phosphorylation (third panel, compare lane 4 with lane 11 and lane 5 with lane 12). Also, PKRΔ6 did not affect PERK phosphorylation on Thr980 (top panel). These data further substantiate the notion that eIF2α phosphorylation is mediated by both PERK and PKR upon VSV infection and that a cross talk between both kinases is necessary to inhibit viral replication.

PERK modulates dsRNA-mediated PKR activation. One of the mechanisms proposed to activate PKR during virus infection is the dimerization of the kinase upon dsRNA binding (22). Since dsRNA is generated throughout the life cycle of VSV (39), we wanted to investigate whether PERK was capable of modulating PKR activation in cells transfected with dsRNA (Fig. 7). We noticed that the induction of eIF2α phosphorylation was impaired in PERK$^{-/-}$ MEFs upon dsRNA treatment as opposed to PERK$^{+/+}$ cells (Fig. 7A, compare lane 4 with lane 2). The same was observed regarding PKR activation (Fig. 7B). We performed a PKR immunoprecipitation, followed by an in vitro kinase assay, thus revealing that PERK$^{-/-}$ MEFs were incapable of fully activating PKR (Fig. 7B, top panel). To the same extent, phosphorylation of PKR on Thr446 was impaired in the PERK$^{-/-}$ cells (Fig. 7B, middle panel). These results suggested that the efficient activation of PKR by dsRNA required PERK.

DISCUSSION

Our findings demonstrate an important role for PERK in VSV infection. We show that PERK-mediated eIF2α phosphorylation is induced in VSV-infected cells and that this is accompanied by an inhibition of virus replication and apoptosis. PERK also plays an essential role in UPR (31) and, as such, its activation in VSV infection initially indicated an ability of the virus to elicit a UPR. This was consistent with the notion that viruses that use the ER as an integral part of their replication strategy are likely able to induce an ER stress response (1). In fact, previous studies showed that the VSV glycoprotein (VSV-G) oligomerizes in the ER prior to its transport to the cell surface (41). Misfolded and unassembled VSV-G is retained in the ER (8), whereas the interactions of the viral protein with two chaperones, BiP and calnexin, are essential for efficient folding and for retention of partially folded G protein forms in the ER (12). Thus, an overload of VSV-G in the ER during virus replication might have been one of the mechanisms eliciting an ER stress response in infected cells. In contrast to this, we found that expression of various ER stress

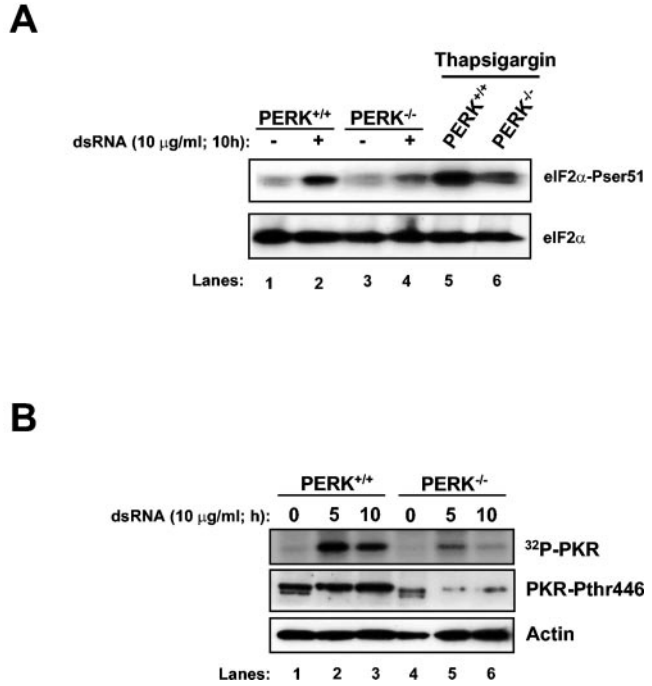

FIG. 7. PKR activation is impaired in dsRNA treated PERK$^{-/-}$ MEFs. (A) PERK$^{+/+}$ and PERK$^{-/-}$ MEFs were transfected with dsRNA (10 μg/ml, lanes 2 and 4) or mock transfected (lanes 1 and 3) or treated with TG (1 μM, 2 h; lanes 5 and 6). Proteins extracts were harvested at the indicated times and subjected to immunoblot analysis with the serine 51 phospho-specific eIF2α antibody (top panel) or with the eIF2α panspecific antibody (lower panel). (B) Protein extracts (200 μg) from dsRNA transfected PERK$^{+/+}$ and PERK$^{-/-}$ MEFs were immunoprecipitated with a rabbit polyclonal anti-mPKR antibody (D-20) and subjected to phosphorylation in vitro in the presence of [γ-^{32}P]ATP. The immunoprecipitated PKR was subjected to SDS–10% PAGE and autoradiography (top panel). Protein extracts (50 μg) were subjected to immunoblot analysis with a rabbit polyclonal phosphothreonine 446 PKR antibody (second panel) or a mouse monoclonal actin antibody (bottom panel).

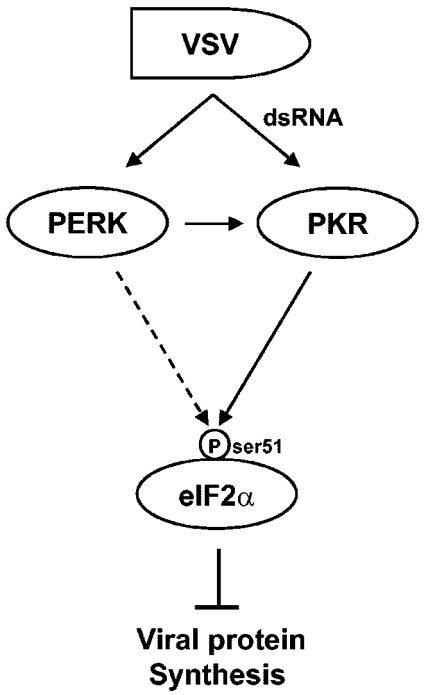

FIG. 8. Model depicting a cross talk between PERK and PKR upon VSV infection. VSV activates both PERK and PKR. Although PKR is thought to be activated by dsRNA produced during virus replication, the molecular mechanism(s) of PERK activation is not clear. Perhaps VSV infection induces protein phosphorylation cascades, resulting in PERK phosphorylation in the ER. PERK is upstream of PKR, and coordinated activation of both kinases is likely to be required for maximal eIF2α phosphorylation and full-scale shutdown of viral protein synthesis (solid lines). Phosphorylation of eIF2α mediated by PERK alone may not be sufficient to block virus replication (dotted line) unless PKR is present (solid lines). This is consistent with the impaired antiviral response of PKR$^{-/-}$ MEFs after VSV infection (2, 37).

markers, including CHOP, BiP, or XBP-1, was not induced in infected cells, nor was their expression impaired in PERK$^{-/-}$ MEFs (unpublished data). As such, we concluded that VSV utilizes a novel pathway to activate PERK. Although this pathway is not currently known, we hypothesize that virus infection might induce protein phosphorylation cascades, leading to the activation of PERK in the ER.

Our data show that inhibition of VSV replication is mediated by the direct phosphorylation of eIF2α by PERK. However, it remains possible that additional control mechanisms are modulated by PERK in VSV-infected cells. In fact, we demonstrate that activation of PKR is impaired in cells lacking PERK, suggesting a functional cross talk between the two kinases with PKR functioning downstream of PERK. Previous data showed that treatment of cells with TG and TNF-α renders PKR active providing evidence for a role of the kinase in ER stress (29, 35). More recent research indicated that ER-stressed cells can induce the activation and nuclear translocation of PKR (25). Consistent with these findings, our data show the induction of PKR in ER-stressed cells and the lack of its activation in PERK$^{-/-}$ cells (Fig. 6D). At present, we do not know how PKR becomes activated by PERK. One possibility is that active PERK directly phosphorylates and activates PKR in the proximity of the ER. Alternatively, activation of PKR is mediated by another kinase that functions as an intermediate between the two eIF2α kinases (Fig. 8). Some data have shown that the cellular inhibitor of PKR, P58IPK (28), can also interact with and inhibit PERK upon ER stress (38, 40). This raises the possibility that the impaired PKR activation observed in ER-stressed PERK$^{-/-}$ MEFs may be explained by the induction of unbound P58IPK. The lack of PERK in these cells may release more P58IPK to the cytoplasm, where it can target and further inhibit PKR. However, it is not yet known whether VSV infection regulates P58IPK expression.

Regarding VSV-mediated apoptosis, our data implicate caspase-12 in this process. It was reported that upon ER stress, the cytosolic caspase-7 translocates to the ER surface and associates with procaspase-12, thereby cleaving its prodomain to generate an active caspase-12 (30). Interestingly, VSV infection was shown to lead to the activation of caspase-7 (16), and this may account, at least in part, for caspase-12 activation in infected cells. Previous findings have shown that caspase-12 has been implicated in apoptosis induced by bovine viral diarrhea virus infection (19), indicating that this protease may play a role in virus-induced apoptosis in mouse cells. When

$PERK^{+/+}$ and $PERK^{-/-}$ MEFs were treated with general caspase inhibitors prior to VSV infection, $PERK^{+/+}$ cells were rescued from VSV infection, as demonstrated by the absence of PARP cleavage. This suggested that caspases were involved in VSV-mediated apoptosis. However, $PERK^{-/-}$ MEFs were highly prone to PARP cleavage and VSV infection, despite caspase inhibition. This suggests that, in the absence of PERK, the virus can utilize caspase-independent apoptotic pathways to induce PARP cleavage. This finding demonstrates that multiple caspase-dependent and caspase-independent cell death pathways may be activated during VSV infection and that PERK plays a role in modulating caspase function and activation. It is now understood that PARP is an important activator of caspase-independent cell death (17), and perhaps VSV can exploit some of these pathways to induce apoptosis. Undoubtedly, future experiments are needed to better characterize the fundamental pathways of VSV-induced apoptosis.

We have shown here that PERK appears to be a critical component of the innate immune response protecting the host against VSV infection. It does so, at least in part, through the activation of PKR. Thus, a cross talk between PERK, PKR and possibly other eIF2α kinases is likely to exist and contribute to the antiviral mechanisms converging at the eIF2α phosphorylation level (Fig. 8). Although many viruses have evolved unique mechanisms to overcome PKR activation (20), it appears that some of these mechanisms also aim at inactivating PERK. For example, hepatitis C virus E2 protein (27) and vaccinia virus K3L protein (34) are potent inhibitors of PERK, as is the P58 PKR inhibitor (P58IPK) induced in cells infected with influenza virus (40). Thus, further investigation of the role of the eIF2α kinase family members in virus infection may yield important information about the translational mechanisms of virus replication and lead to the discovery of unique pathways controlled by each of the eIF2α kinases with important implications against virus infection and associated disease.

ACKNOWLEDGMENTS

We thank D. Moraitis for technical assistance and D. Ron and H. Harding for $PERK^{-/-}$ MEFs, PERK, BiP, XBP-1, and CHOP cDNAs and helpful suggestions.

D.B. is a research student of the Terry Fox Foundation through an award from the National Cancer Institute of Canada and a recipient of the CIHR Cancer Consortium Training Grant Studentship Award. This study was supported by a grant from the National Cancer Institute of Canada awarded to A.E.K. A.E.K. is a recipient of a Scientist Award from CIHR.

REFERENCES

1. **Aridor, M., and W. E. Balch.** 1999. Integration of endoplasmic reticulum signaling in health and disease. Nat. Med. **5:**745–751.
2. **Balachandran, S., P. C. Roberts, L. E. Brown, H. Truong, A. K. Pattnaik, D. R. Archer, and G. N. Barber.** 2000. Essential role for the dsRNA-dependent protein kinase PKR in innate immunity to viral infection. Immunity **13:**129–141.
3. **Baltzis, D., S. Li, and A. E. Koromilas.** 2002. Functional characterization of *pkr* gene products expressed in cells from mice with a targeted deletion of the N terminus or C terminus domain of PKR. J. Biol. Chem. **277:**38364–38372.
4. **Bitko, V., and S. Barik.** 2001. An endoplasmic reticulum-specific stress-activated caspase (caspase-12) is implicated in the apoptosis of A549 epithelial cells by respiratory syncytial virus. J. Cell Biochem. **80:**441–454.
5. **Chen, J. J.** 2000. Heme-regulated eIF2α kinase, p. 529–546. *In* N. Sonenberg, J. W. B. Hershey, and M. B. Mathews (ed.), Translational control of gene expression. Cold Spring Harbor Laboratory Press, Cold Spring Harbor, N.Y.
6. **Chu, W. M., D. Ostertag, Z. W. Li, L. Chang, Y. Chen, Y. Hu, B. Williams, J. Perrault, and M. Karin.** 1999. JNK2 and IKKβ are required for activating the innate response to viral infection. Immunity **11:**721–731.
7. **Desforges, M., G. Despars, S. Berard, M. Gosselin, M. O. McKenzie, D. S. Lyles, P. J. Talbot, and L. Poliquin.** 2002. Matrix protein mutations contribute to inefficient induction of apoptosis leading to persistent infection of human neural cells by vesicular stomatitis virus. Virology **295:**63–73.
8. **de Silva, A. M., W. E. Balch, and A. Helenius.** 1990. Quality control in the endoplasmic reticulum: folding and misfolding of vesicular stomatitis virus G protein in cells and in vitro. J. Cell Biol. **111:**857–866.
9. **Dever, T. E.** 2002. Gene-specific regulation by general translation factors. Cell **108:**545–556.
10. **Donze, O., R. Jagus, A. E. Koromilas, J. W. Hershey, and N. Sonenberg.** 1995. Abrogation of translation initiation factor eIF-2 phosphorylation causes malignant transformation of NIH 3T3 cells. EMBO J. **14:**3828–3834.
11. **Durbin, R. K., S. E. Mertz, A. E. Koromilas, and J. E. Durbin.** 2002. PKR protection against intranasal vesicular stomatitis virus infection is mouse strain dependent. Viral Immunol. **15:**41–51.
12. **Hammond, C., and A. Helenius.** 1994. Folding of VSV G protein: sequential interaction with BiP and calnexin. Science **266:**456–458.
13. **Harding, H. P., M. Calfon, F. Urano, I. Novoa, and D. Ron.** 2002. Transcriptional and translational control in the mammalian unfolded protein response. Annu. Rev. Cell Dev. Biol. **18:**575–599.
14. **Harding, H. P., Y. Zhang, and D. Ron.** 1999. Protein translation and folding are coupled by an endoplasmic-reticulum-resident kinase. Nature **397:**271–274.
15. **Hershey, J. W.** 1991. Translational control in mammalian cells. Annu. Rev. Biochem. **60:**717–755.
16. **Hobbs, J. A., R. H. Schloemer, G. Hommel-Berrey, and Z. Brahmi.** 2001. Caspase-3-like proteases are activated by infection but are not required for replication of vesicular stomatitis virus. Virus Res. **80:**53–65.
17. **Hong, S. J., T. M. Dawson, and V. L. Dawson.** 2004. Nuclear and mitochondrial conversations in cell death: PARP-1 and AIF signaling. Trends Pharmacol. Sci. **25:**259–264.
18. **Iordanov, M. S., J. M. Paranjape, A. Zhou, J. Wong, B. R. Williams, E. F. Meurs, R. H. Silverman, and B. E. Magun.** 2000. Activation of p38 mitogen-activated protein kinase and c-Jun NH_2-terminal kinase by double-stranded RNA and encephalomyocarditis virus: involvement of RNase L, protein kinase R, and alternative pathways. Mol. Cell. Biol. **20:**617–627.
19. **Jordan, R., L. Wang, T. M. Graczyk, T. M. Block, and P. R. Romano.** 2002. Replication of a cytopathic strain of bovine viral diarrhea virus activates PERK and induces endoplasmic reticulum stress-mediated apoptosis of MDBK cells. J. Virol. **76:**9588–9599.
20. **Katze, M. G., Y. He, and M. Gale, Jr.** 2002. Viruses and interferon: a fight for supremacy. Nat. Rev. Immunol. **2:**675–687.
21. **Kaufman, R. J.** 1999. Double-stranded RNA-activated protein kinase mediates virus-induced apoptosis: a new role for an old actor. Proc. Natl. Acad. Sci. USA **96:**11693–11695.
22. **Kaufman, R. J.** 2000. The double-stranded RNA-activated protein kinase PKR, p. 503–527. *In* N. Sonenberg, J. W. B. Hershey, and M. B. Mathews (ed.), Translational control of gene expression. Cold Spring Harbor Laboratory Press, Cold Spring Harbor, N.Y.
23. **Kimball, S. R., and L. S. Jefferson.** 2000. Regulation of translation initiation in mammalian cells by amino acids, p. 561–579. *In* N. Sonenberg, J. W. B. Hershey, and M. B. Mathews (ed.), Translational control of gene expression. Cold Spring Harbor Laboratory Press, Cold Spring Harbor, N.Y.
24. **Nakagawa, T., H. Zhu, N. Morishima, E. Li, J. Xu, B. A. Yankner, and J. Yuan.** 2000. Caspase-12 mediates endoplasmic-reticulum-specific apoptosis and cytotoxicity by amyloid-beta. Nature **403:**98–103.
25. **Onuki, R., Y. Bando, E. Suyama, T. Katayama, H. Kawasaki, T. Baba, M. Tohyama, and K. Taira.** 2004. An RNA-dependent protein kinase is involved in tunicamycin-induced apoptosis and Alzheimer's disease. EMBO J. **23:**959–968.
26. **Oyadomari, S., E. Araki, and M. Mori.** 2002. Endoplasmic reticulum stress-mediated apoptosis in pancreatic beta-cells. Apoptosis **7:**335–345.
27. **Pavio, N., P. R. Romano, T. M. Graczyk, S. M. Feinstone, and D. R. Taylor.** 2003. Protein synthesis and endoplasmic reticulum stress can be modulated by the hepatitis C virus envelope protein E2 through the eukaryotic initiation factor 2α kinase PERK. J. Virol. **77:**3578–3585.
28. **Polyak, S. J., N. Tang, M. Wambach, G. N. Barber, and M. G. Katze.** 1996. The P58 cellular inhibitor complexes with the interferon-induced, double-stranded RNA-dependent protein kinase, PKR, to regulate its autophosphorylation and activity. J. Biol. Chem. **271:**1702–1707.
29. **Prostko, C. R., J. N. Dholakia, M. A. Brostrom, and C. O. Brostrom.** 1995. Activation of the double-stranded RNA-regulated protein kinase by depletion of endoplasmic reticular calcium stores. J. Biol. Chem. **270:**6211–6215.
30. **Rao, R. V., E. Hermel, S. Castro-Obregon, G. del Rio, L. M. Ellerby, H. M. Ellerby, and D. E. Bredesen.** 2001. Coupling endoplasmic reticulum stress to the cell death program: mechanism of caspase activation. J. Biol. Chem. **276:**33869–33874.
31. **Ron, D., and H. P. Harding.** 2000. PERK and translational control by stress in the endoplasmic reticulum, p. 547–560. *In* N. Sonenberg, J. W. B. Hershey, and M. B. Mathews (ed.), Translational control of gene expression. Cold Spring Harbor Laboratory Press, Cold Spring Harbor, N.Y.
32. **Sambrook, J., E. F. Fritsch, and T. Maniatis.** 1989. Molecular cloning: a

laboratory manual, 2nd ed. Cold Spring Harbor Laboratory Press, Plainview, N.Y.

33. **Sharma, S., B. R. TenOever, N. Grandvaux, G. P. Zhou, R. Lin, and J. Hiscott.** 2003. Triggering the interferon antiviral response through an IKK-related pathway. Science **300:**1148–1151.
34. **Sood, R., A. C. Porter, K. Ma, L. A. Quilliam, and R. C. Wek.** 2000. Pancreatic eukaryotic initiation factor-2α kinase (PEK) homologues in humans, *Drosophila melanogaster* and *Caenorhabditis elegans* that mediate translational control in response to endoplasmic reticulum stress. Biochem. J. **346**(Pt. 2)**:**281–293.
35. **Srivastava, S. P., K. U. Kumar, and R. J. Kaufman.** 1998. Phosphorylation of eukaryotic translation initiation factor 2 mediates apoptosis in response to activation of the double-stranded RNA-dependent protein kinase. J. Biol. Chem. **273:**2416–2423.
36. **Stark, G. R., I. M. Kerr, B. R. Williams, R. H. Silverman, and R. D. Schreiber.** 1998. How cells respond to interferons. Annu. Rev. Biochem. **67:**227–264.
37. **Stojdl, D. F., N. Abraham, S. Knowles, R. Marius, A. Brasey, B. D. Lichty, E. G. Brown, N. Sonenberg, and J. C. Bell.** 2000. The murine double-stranded RNA-dependent protein kinase PKR is required for resistance to vesicular stomatitis virus. J. Virol. **74:**9580–9585.
38. **Van Huizen, R., J. L. Martindale, M. Gorospe, and N. J. Holbrook.** 2003. P58IPK, a novel endoplasmic reticulum stress-inducible protein and potential negative regulator of eIF2α signaling. J. Biol. Chem. **278:**15558–15564.
39. **Wagner, R. R., and J. K. Rose.** 1996. *Rhabdoviridae*: the viruses and their replication, p. 1121–1135. *In* B. N. Fields, D. M. Knipe, and P. M. Howley (ed.), Fields virology, vol. 1. Lippincott-Raven Publishers, Philadelphia, Pa.
40. **Yan, W., C. L. Frank, M. J. Korth, B. L. Sopher, I. Novoa, D. Ron, and M. G. Katze.** 2002. Control of PERK eIF2α kinase activity by the endoplasmic reticulum stress-induced molecular chaperone P58IPK. Proc. Natl. Acad. Sci. USA **99:**15920–15925.
41. **Zagouras, P., A. Ruusala, and J. K. Rose.** 1991. Dissociation and reassociation of oligomeric viral glycoprotein subunits in the endoplasmic reticulum. J. Virol. **65:**1976–1984.